IEEE Access
Multidisciplinary ⋮ Rapid Review ⋮ Open Access Journal

Received 28 January 2026, accepted 17 February 2026, date of publication 25 February 2026, date of current version 5 March 2026.

Digital Object Identifier 10.1109/ACCESS.2026.3667732

RESEARCH ARTICLE

A Soft Fabric-Based Thermal Haptic Device for Virtual Reality

RUI CHEN[1], (Student Member, IEEE), XIANLONG MAI[1,2], DOMENICO CHIARADIA[1], ANTONIO FRISOLI[1], (Senior Member, IEEE), AND DANIELE LEONARDIS[1]

[1]Institute of Mechanical Intelligence, Department of Excellence in Robotics and AI, School of Advanced Studies Sant'Anna (SSSA), 56127 Pisa, Italy
[2]CAS Key Laboratory of Mechanical Behavior and Design of Materials, Institute of Humanoid Robots, School of Engineering Sciences, University of Science and Technology of China, Hefei 230026, China

Corresponding author: Rui Chen (rui.chen@santannapisa.it)

This work was supported in part by the BRIEF Project "Biorobotics Research and Innovation Engineering Facilities" funded through the National Recovery and Resilience Plan (NRRP), Mission 4: "Istruzione e Ricerca," Component 2: "Dalla ricerca all'impresa," under Project IR0000036; and in part by the Investment 3.1: "Fondo per la realizzazione di un sistema integrato di infrastrutture di ricerca e innovazione," funded by European Union–NextGenerationEU under Grant J13C22000400007.

ABSTRACT This article presents a novel fabric-based thermal-haptic interface for virtual reality. It integrates pneumatic actuation and conductive fabric with an innovative ultra-lightweight design, achieving only 2 g for each finger unit. By embedding heating elements within textile pneumatic chambers, the system delivers modulated pressure and thermal stimuli to fingerpads through a fully soft, wearable interface. Comprehensive characterization demonstrates rapid thermal modulation with heating rates up to 3°C/s, enabling dynamic thermal feedback for virtual interactions. The pneumatic subsystem generates forces up to 8.93 N at 50 kPa, while optimization of fingerpad-actuator clearance enhances cooling efficiency with minimal force reduction. Experimental validation conducted with two different user studies shows high temperature identification accuracy (0.98 overall) across three thermal levels and significant manipulation improvements in a virtual pick-and-place task. Results show enhanced success rates (88.5% to 96.4%, $p = 0.029$) and improved force control precision ($p = 0.013$) when haptic feedback is enabled, validating the effectiveness of the integrated thermal-haptic approach for advanced human-machine interaction applications.

INDEX TERMS Haptics, soft robotics, pneumatic actuators, thermal feedback, virtual reality, wearable device.

I. INTRODUCTION

Haptic feedback constitutes a critical component in virtual reality (VR) applications, providing rich sensory information that enables complex task execution and enhances user immersion [1], [2], [3]. Modern haptic systems integrate various actuators into wearable devices to deliver comprehensive tactile sensations, including pressure, vibration, deformation, texture, and temperature, effectively simulating real-world interactions [4].

Pneumatic actuators have emerged as a promising solution for haptic feedback delivery, offering significant advantages in weight reduction, inherent compliance, and cost-effectiveness [5], [6], [7], [8]. Recent advances in rubber-based pneumatic systems have demonstrated successful sensor integration for closed-loop control [9], while their expansive volume capabilities enable substantial tactile variations [10], [11], [12], [13]. Within this domain, fabric-based pneumatic actuators have gained particular attention due to their minimal weight and manufacturing simplicity, exemplified by innovations such as pouch motors [14], [15]. Notable implementations include WRAP, a four-motor pneumatic system for directional guidance in medical interventions [16], systems creating continuous lateral motion sensations through coordinated actuation [17], and devices simulating handshake sensations via strategically positioned actuators [18].

Thermal feedback represents another crucial dimension in haptic interfaces, leveraging the skin's dense thermoreceptor network capable of detecting precise temperature variations.

The associate editor coordinating the review of this manuscript and approving it for publication was Tommaso Lisini Baldi.

This sensory capability provides essential environmental information, driving the development of various thermal haptic devices based on different heat transfer mechanisms [19], [20], [21], [22], [23].

Tactile sensory substitution offers potential for symbolic thermal feedback, yet these technologies remain constrained by difficulties in replicating authentic thermal sensations [24], [25]. Fluid-based thermal systems employ temperature-controlled reservoirs with valve-controlled mixing of hot and cold fluids, enabling precise temperature regulation through flow ratio modulation [26]. However, these systems present design complexities and require stable temperature maintenance. Fluid selection involves trade-offs: water-based systems increase weight, while air-based systems exhibit slower thermal response [27], [28].

Thermoelectric (Peltier) devices represent a widely adopted approach, creating temperature differentials through current flow and enabling precise bidirectional temperature control [19], [29]. While successfully integrated with both motorized [30], [31], [32] and pneumatic systems [33], [34], [35] to provide rapid responses and broad temperature ranges, they face significant challenges including heat accumulation, weight, rigidity, and system complexity [19], [36]. Recent advances in flexible thermoelectric devices have substantially improved module flexibility, yet limitations remain in the efficiency of these devices [37], [38], [39], [40].

Motivated by the need for enhanced compactness, compliance, and wearability in thermal haptic interfaces, we present a fully fabric-based thermal and pneumatic haptic system featuring fabric-based thermal haptic actuators (FTHAs). Each FTHA integrates a pneumatic pouch motor with a fabric electric heater, delivering congruent haptic and thermal feedback to fingertips. While currently limited to heating capabilities, the system achieves exceptional thinness, lightness, and compliance with rapid dynamic response characteristics.

This paper presents comprehensive FTHA characterization, including thermal step response and force output analysis, alongside user studies evaluating device effectiveness in VR applications. Our findings demonstrate that this novel approach could significantly impact VR interfaces, particularly for applications requiring lightweight, compliant, and responsive thermal haptic feedback.

II. SOFT THERMAL HAPTIC DEVICE

The proposed soft thermal haptic device integrates two FTHAs within a wearable wrist strap system, worn on the index finger and thumb, as illustrated in Fig. 1. The FTHAs deliver congruent haptic and thermal feedback to users' fingertips, creating a multimodal tactile experience that is more informative of the virtual or remote interaction. The device employs an ergonomic wrist strap design that efficiently manages pneumatic tubes and electrical connections while ensuring stable positioning during use. The FTHAs mount on the index finger and thumb through elastic fabric interfaces, accommodating various finger sizes.

A key innovation is the ultra-lightweight construction, achieving a mass of only 2 g per FTHA, representing a substantial reduction compared to conventional electromagnetic motor-based haptic systems. Typically, fingertip haptic devices range from 10 to 50 g, depending on the type of actuators [41] and the intensity of the feedback. This minimal mass is crucial for prolonged-use applications, such as VR training simulations or therapeutic interventions, substantially reducing user fatigue while maintaining optimal haptic performance [6].

A. FTHA ARCHITECTURE

The FTHA integrates two primary functional subsystems: a pneumatic pouch actuator for normal force modulation and an electric heating system for thermal sensation, as detailed in Fig. 2(a). The design follows key guidelines, including thermal operation within a comfortable range (25–50°C) with precise control (±1°C), perceptible haptic feedback (greater than 1 N force), and lightweight construction on fingertips (fabrics with a denier of 40D or less are recommended).

The pneumatic subsystem utilizes dual-layer fabric sheets with Thermoplastic Polyurethane (TPU) coating. When pressurized, the pouch motor generates normal force against the fingertip while conforming to the finger's natural contour.

The thermal subsystem integrates a fabric-based electric circuit with an NTC thermistor for temperature sensing, placed on the same layer as the conductive fabric. The conductive fabric element, fabricated with precise laser cutting, generates controlled heat when current is applied due to the Joule effect. A closed-loop PID controller (Kp = 10, Ki = 1, Kd = 5) is implemented to maintain the desired temperature. A temperature deadband of 0.2°C (no control action is taken when the temperature remains within ±0.2°C of the setpoint) is applied to prevent frequent switching, reduce oscillations, and improve system reliability and lifetime. To prevent potential finger burns from excessive heat, the system incorporates a safety mechanism that sets the maximum allowable temperature at 50°C; heating is immediately terminated if this threshold is exceeded. While heating is actively controlled, cooling relies on passive mechanisms that include natural convection and thermal dissipation through the device structure.

B. FABRICATION METHODOLOGY

The fabrication process follows a systematic approach to ensure consistent device performance and reliability. Precision laser cutting produces the required components: two rectangular TPU-coated fabric sections (Adventure Experts, Slovenia, 40-denier) and a square woven conductive fabric circuit. A supplementary TPU film facilitates component integration, as shown in Fig. 2(a).

Assembly begins with precise positioning and thermal bonding of the NTC thermistor (50 kΩ at 25°C) and fabric circuit onto one TPU-coated fabric layer using the prepared TPU film (Fig. 2(b)). The second TPU-coated fabric layer

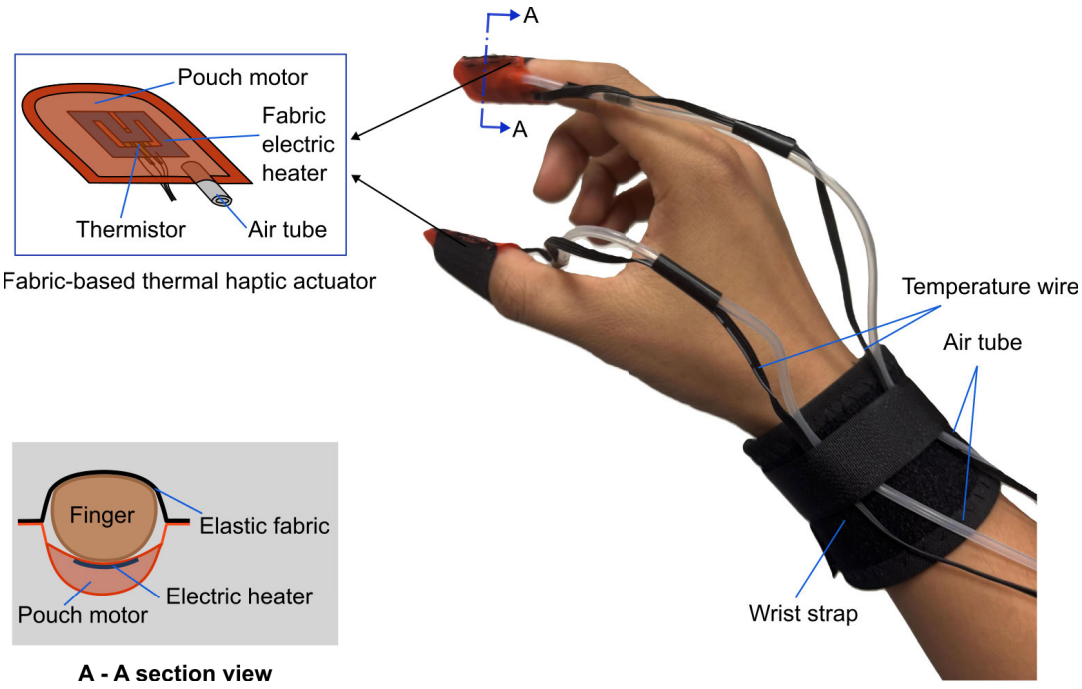

FIGURE 1. Conceptual illustration of the proposed soft fabric-based thermal haptic device integrating dual-modal feedback capabilities for fingertip interaction.

is then heat-sealed to the circuit-integrated layer, forming the pneumatic pouch motor structure. A TPU air tube is bonded using cyanoacrylate adhesive to enable pneumatic control (Fig. 2(c)). Final assembly involves sewing an elastic fabric interface to create an ergonomic fingertip attachment (Fig. 2(d)).

Critical design parameters were optimized for thermal and haptic performance. The conductive circuit dimensions (15 mm × 15 mm) provide adequate fingertip contact area, with 3 mm-wide circuit traces ensuring uniform current distribution. The thermistor's central placement allows accurate temperature measurement of the active area. Pouch actuator dimensions were chosen based on average finger anthropometrics: 18 mm (breadth) × 16 mm for the index finger and 20 mm (breadth) × 18 mm for the thumb, ensuring reliable contact across diverse user populations [42].

C. THERMAL RESPONSE CHARACTERIZATION

The FTHA control system architecture (Fig. 4(a)) features an ESP-32 microcontroller serving as the central control system for the FTHAs. Two high-precision proportional solenoid valves (ITV0010, SMC Corporation) regulate compressed air supply to the pouch motors, achieving precise pressure modulation and corresponding force output control. Fabric heater operation is managed through sophisticated current control utilizing an H-bridge driver IC configuration, enabling precise power regulation. Temperature feedback utilizes NTC thermistor resistance measurements integrated within a closed-loop PID controller framework to maintain desired temperature setpoints with exceptional accuracy.

A comprehensive thermal characterization study was conducted to evaluate the device's temperature control capabilities under both unloaded and finger-contact conditions. The experimental protocol employed a series of step input signals from 25°C to 40°C, each lasting 40 seconds. Temperature data was acquired at 5 Hz sampling rate, enabling detailed analysis of thermal dynamics as illustrated in Fig. 3(b).

Under unloaded conditions, the actuator exhibited rapid initial heating with a peak heating rate of approximately 3°C/s during the initial phase, attributed to maximum temperature differential. The system achieved the target temperature of 40°C within 8.4 seconds, demonstrating an average heating rate of 1.79°C/s. The cooling phase exhibited notably different dynamics, requiring approximately 90 seconds to return to baseline temperature with a maximum cooling rate of 0.4°C/s during the initial cooling period. Thermal imaging revealed distinct coil patterns during temperature rise due to large gradients between the heated coil and surrounding fabric (Fig. 3(c)), which became diffused as temperature approached steady state (Fig. 3(d)).

Under finger-contact conditions, thermal behavior demonstrated significant modifications due to bio-thermal interactions. The baseline temperature stabilized at approximately 34°C, reflecting thermal equilibrium between the actuator and finger tissue. The heating phase from 34°C to 40°C required 7.6 seconds, achieving an average heating rate of 0.79°C/s. The cooling phase exhibited significantly extended duration, requiring approximately 70 seconds to return to the finger-contact baseline temperature—a substantial difference compared to unloaded conditions.

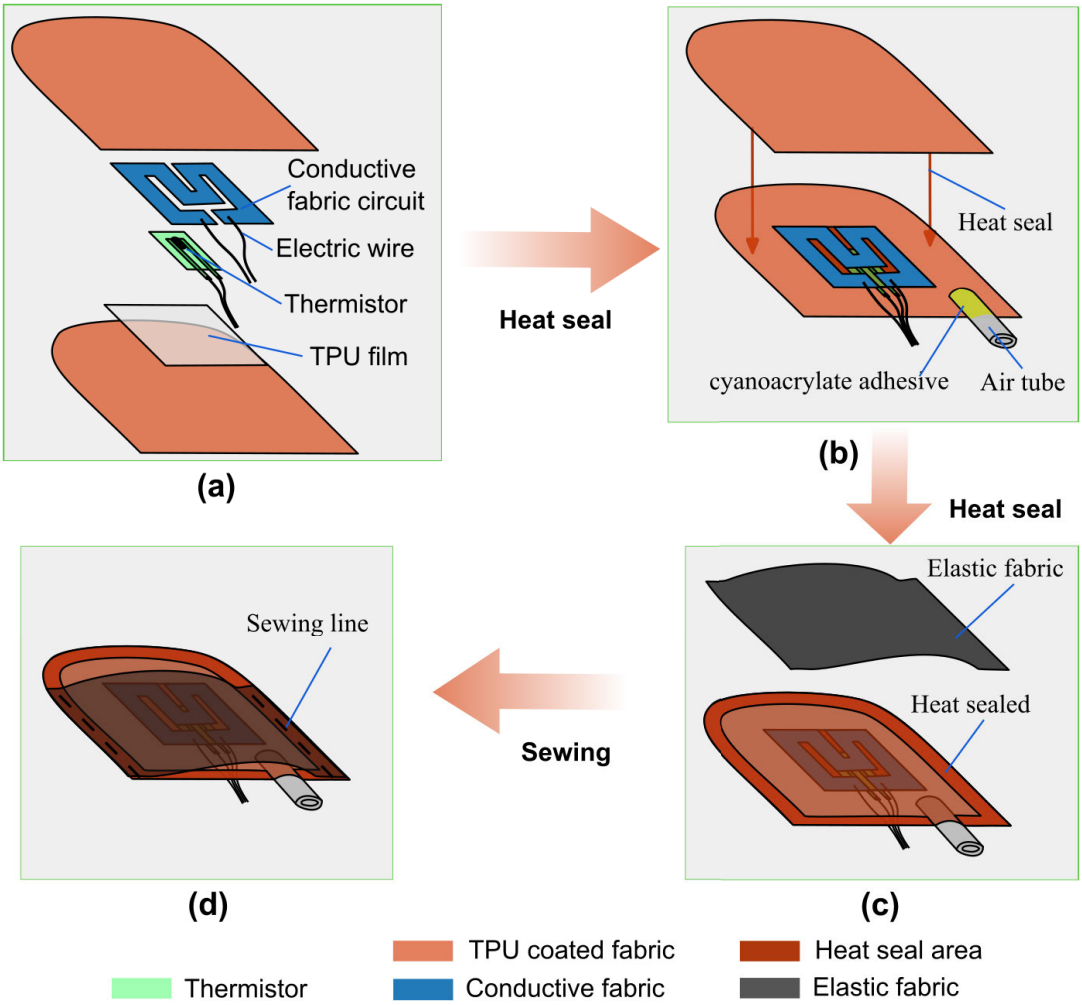

FIGURE 2. FTHA fabrication process: (a) component preparation including TPU-coated fabrics and conductive circuit, (b) integration of thermistor and conductive fabric circuit, (c) heat-sealing of pneumatic chamber with air tube attachment, (d) final assembly with elastic fabric interface.

This observed disparity in cooling rates between contact and non-contact conditions reveals a critical design consideration for thermal haptic systems. The enhanced cooling efficiency in unloaded states suggests that the strategic implementation of a controlled clearance between finger and actuator during deflated states could significantly improve thermal responsiveness. This finding indicates that optimizing the actuator-fingerpad gap when thermal feedback is not required could enhance overall system performance by facilitating more rapid thermal state transitions while maintaining effective force transmission during inflated states.

D. FORCE CHARACTERIZATION AND CLEARANCE OPTIMIZATION

Building upon thermal characterization findings that demonstrated enhanced cooling rates with increased actuator-finger clearance, a comprehensive force characterization study was conducted to quantify the trade-off between thermal performance and force output capabilities. A specialized experimental apparatus was developed to systematically evaluate FTHA force output characteristics under varying clearance conditions, as illustrated in Fig. 4(a) and (b).

The testing platform comprises five key components: an anatomically-curved top plate, dual precision adjustment screws, connector assembly, high-precision force sensor, and contoured base plate. The curved profiles of both plates were engineered to replicate geometric constraints of human fingertip interaction, enabling accurate simulation of force transfer dynamics during actual device operation. The dual adjustment screws facilitate precise clearance control between the deflated actuator and top plate, enabling systematic investigation of clearance effects on force output characteristics.

The experimental protocol began with precise calibration of the initial contact state. Adjustment screws were carefully manipulated until a minimal preloading force of 0.05 N was measured by the force sensor, establishing the zero-clearance (D = 0 mm) reference position. Subsequent force measurements were conducted by incrementally increasing the input pressure from 0 to 50 kPa while

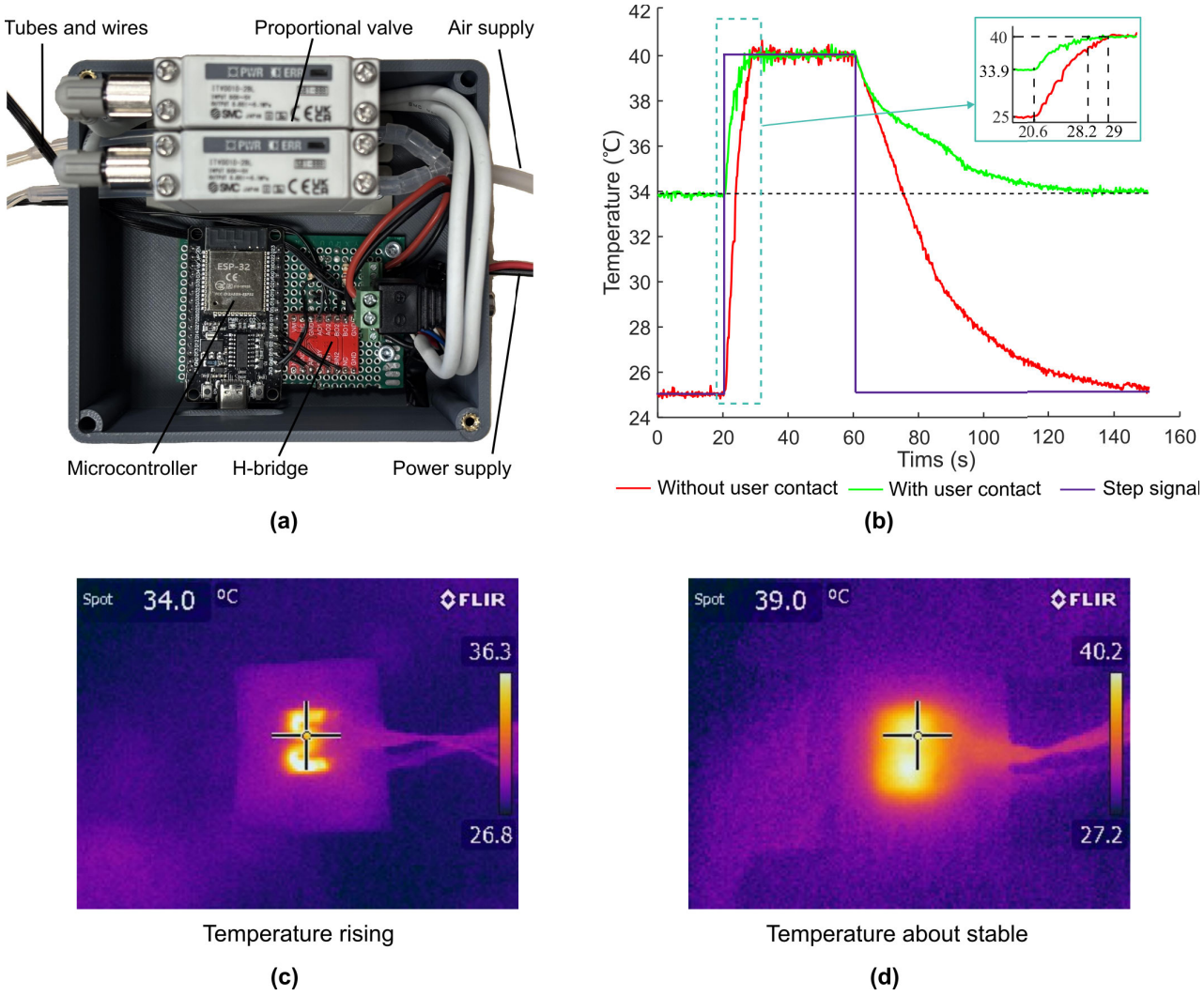

FIGURE 3. Thermal characterization of FTHAs: (a) control system configuration for thermal characterization studies, (b) temperature step response under unloaded and finger-contact conditions, (c) thermal image during temperature rise showing distinct coil heating pattern, (d) thermal image near steady state showing diffused heat distribution.

simultaneously recording pressure and force data. This procedure was systematically repeated across multiple clearance settings (D = 0, 1, 2, and 3 mm) to characterize the relationship between clearance, input pressure, and output force.

The experimental results, presented in Fig. 4(c), demonstrate a predominantly linear relationship between input pressure and output force across all tested clearance values. Maximum force output of 8.93 N was achieved at 50 kPa with D = 0 mm. Systematic but moderate decreases in maximum force output were observed with increasing clearance values. Specifically, clearances of 1 mm, 2 mm, and 3 mm yielded maximum force outputs of approximately 8.5 N (5% reduction), 7.7 N (14% reduction), and 6.6 N (26% reduction), respectively. It should be noted that the rigid curved plates used in this testing setup may overestimate the practical force output compared to actual finger contact, as deformable finger tissue would distribute and absorb forces differently.

Pressure step response tests were conducted to characterize the actuation time. Three pressure levels—10 kPa, 30 kPa, and 50 kPa—were applied for 3 seconds, and then the pressure was set to zero again. With the SMC ITV0010 proportional regulator and its integrated pressure sensor, the actual actuation pressure can be both controlled and measured through analog signals (0–5V corresponding to 0–100 kPa). The sampling frequency for the pneumatic actuation was 95 Hz. The result is shown in Fig. 4(d). For 50 kPa pressure, the rise time (the time required to raise the value from 10% to 90%) was 0.25 s. It is also worth noting that the actuation time of a pneumatic actuator relies heavily on the air supply system—a higher flow rate value and tube can improve the response speed.

III. USER STUDY

A. SYSTEM OVERVIEW

Two user studies were conducted to investigate thermal haptic device performance. A user study combining

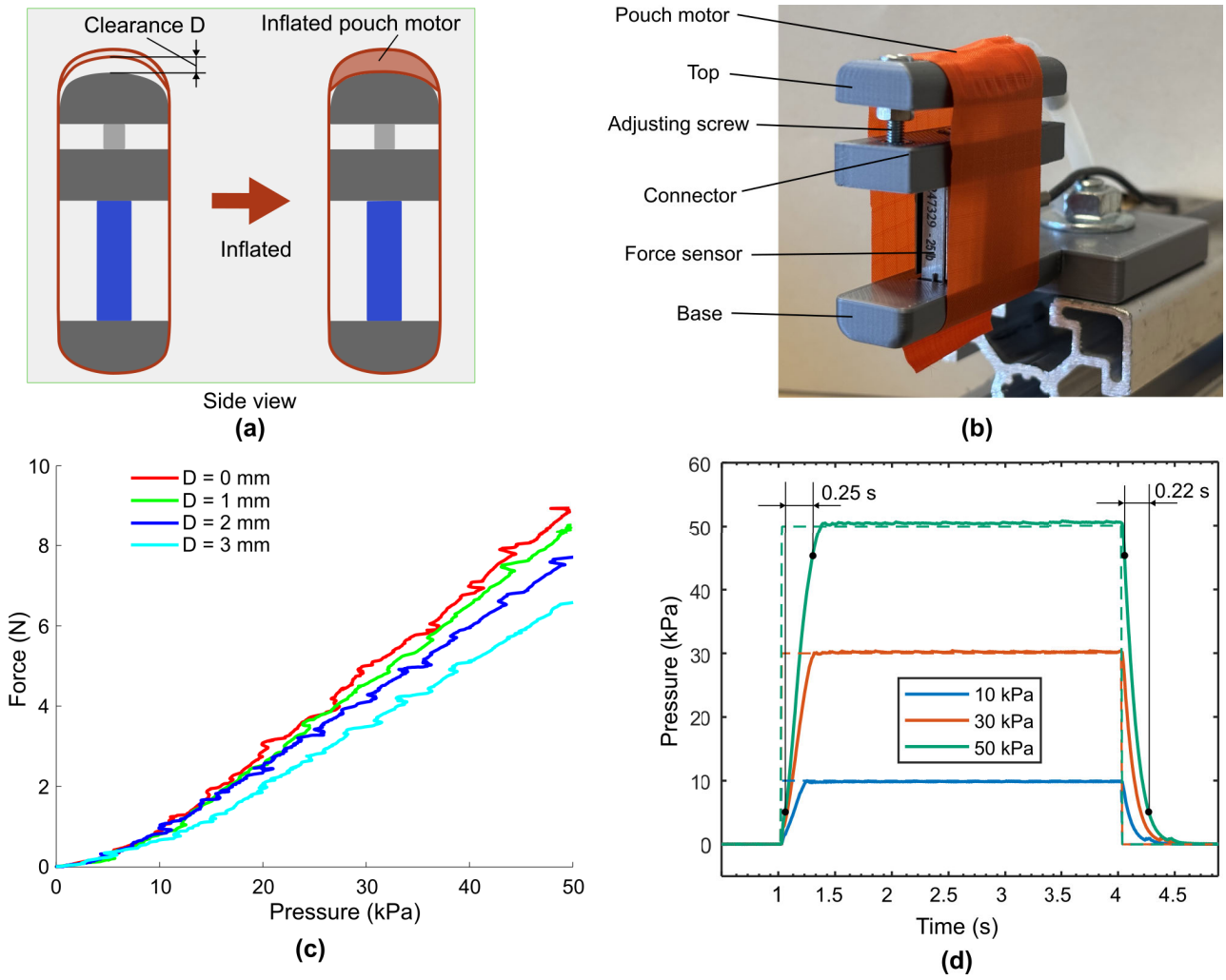

FIGURE 4. Force characterization of FTHAs: (a) experimental setup with anatomically-curved testing platform, (b) schematic diagram showing clearance control mechanism, (c) force output versus input pressure under different clearance conditions.

thermal and haptic feedback is detailed in Appendix A (Figs.7-8). The main experimental evaluation separated thermal feedback (temperature discrimination) and haptic feedback (virtual manipulation) protocols as described below.

Eleven healthy subjects participated in the experiments (7 male, 4 female; aged 28.8 ± 3.1 years), all right-handed. The study was approved by the Ethical Board of the Scuola Superiore Sant'Anna (protocol 412023), with informed consent obtained from all participants.

B. THERMAL FEEDBACK EXPERIMENT

Three temperature levels were evaluated: cool (25°C, heater off), warm (40–41°C), and hot (43–44°C). These temperatures were selected based on an exploratory test performed by the experimenters and on previous findings [43]: 40–41°C is perceived as comfortably warm, 43–44°C approaches the upper comfort limit (45°C may cause discomfort, as reported by the participants), and 25°C represents ambient room temperature. Subjects distinguished temperatures using fingertip sensation exclusively, as shown in Fig. 5(a).

A 5-minute familiarization period was conducted to present all the temperature stimuli to the subjects. Subsequently, stimuli were presented in randomized order (18 trials in total, 6 per stimulus). After each stimulus, participants were required to indicate which of the three temperatures they perceived (no time limitation). To ensure consistent fingertip-actuator contact, actuators maintained 10 kPa pressure during testing. Between trials, actuators were deflated for approximately 20 seconds to enable natural cooling. Response times were recorded for each trial, encompassing heating, identification, and response recording phases.

C. HAPTIC FEEDBACK EXPERIMENT

A customized VR environment consists of a purple object, a yellow stand, and a small blue target, as shown in Fig. 5(b). The VR-integrated haptic system (Fig. 5(c))

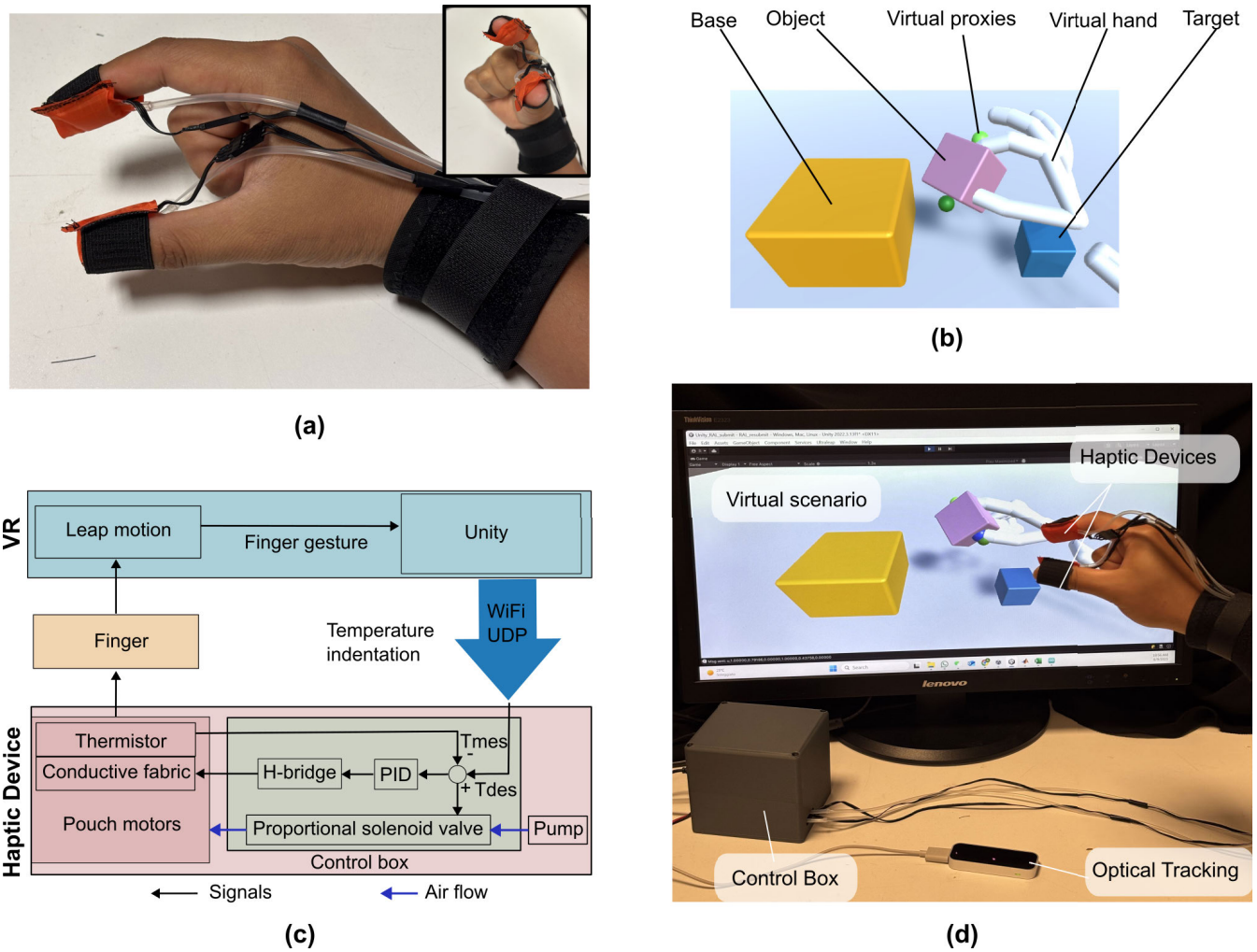

FIGURE 5. Experimental setup: (a) thermal feedback protocol setup, (b) components in VR environment, (c) haptic feedback system schematic showing VR integration, (d) virtual manipulation experimental environment.

employed vision-based hand tracking (Leap Motion, Ultraleap) to capture hand gestures and map them to a virtual hand representation. Virtual hand interactions with objects generated corresponding indentation data transmitted to the haptic device via WiFi using UDP protocol.

The interaction mechanism used fingertip coordinates from the tracking device to control two proxy points in VR. These proxies were connected via virtual springs to virtual spheres (green spheres at fingertips) featuring collisions and physical interaction as rigid bodies in the virtual physics simulation. The implemented virtual spring method [44] enabled modulated object grasping while maintaining stability of the physics simulation, especially during the grasping condition.

In the experimental environment (Fig. 5(d)), the purple object had to be picked from the yellow base and precisely placed on a smaller blue target area. The user could interact with the cube only through the collision-enabled spheres at the index and thumb fingertips. During contact, indentation was calculated as the distance between the tracking proxy and the corresponding collision sphere. The virtual interaction force was proportional to the indentation multiplied by the virtual stiffness coefficient.

Two experimental conditions were evaluated: (1) Haptic Feedback (HF)—subjects wore the haptic device receiving both visual and tactile feedback; (2) No Feedback (NF)—subjects removed the haptic device and manipulated objects with visual feedback only. Pneumatic pressure (the SMC ITV0010 proportional regulator controls the output pressure proportionally to an electrical input signal) was proportional to indentation, up to 20 kPa at 20 mm maximum indentation. For subjects with smaller fingers, additional soft fabric padding was placed between the finger and elastic fabric to ensure proper actuator contact.

Subjects performed object grasping and placement tasks on targets for 15 trials per condition. Successful placement required maintaining object stability on the target for 1 second. Object falls resulted in failed attempts. Condition

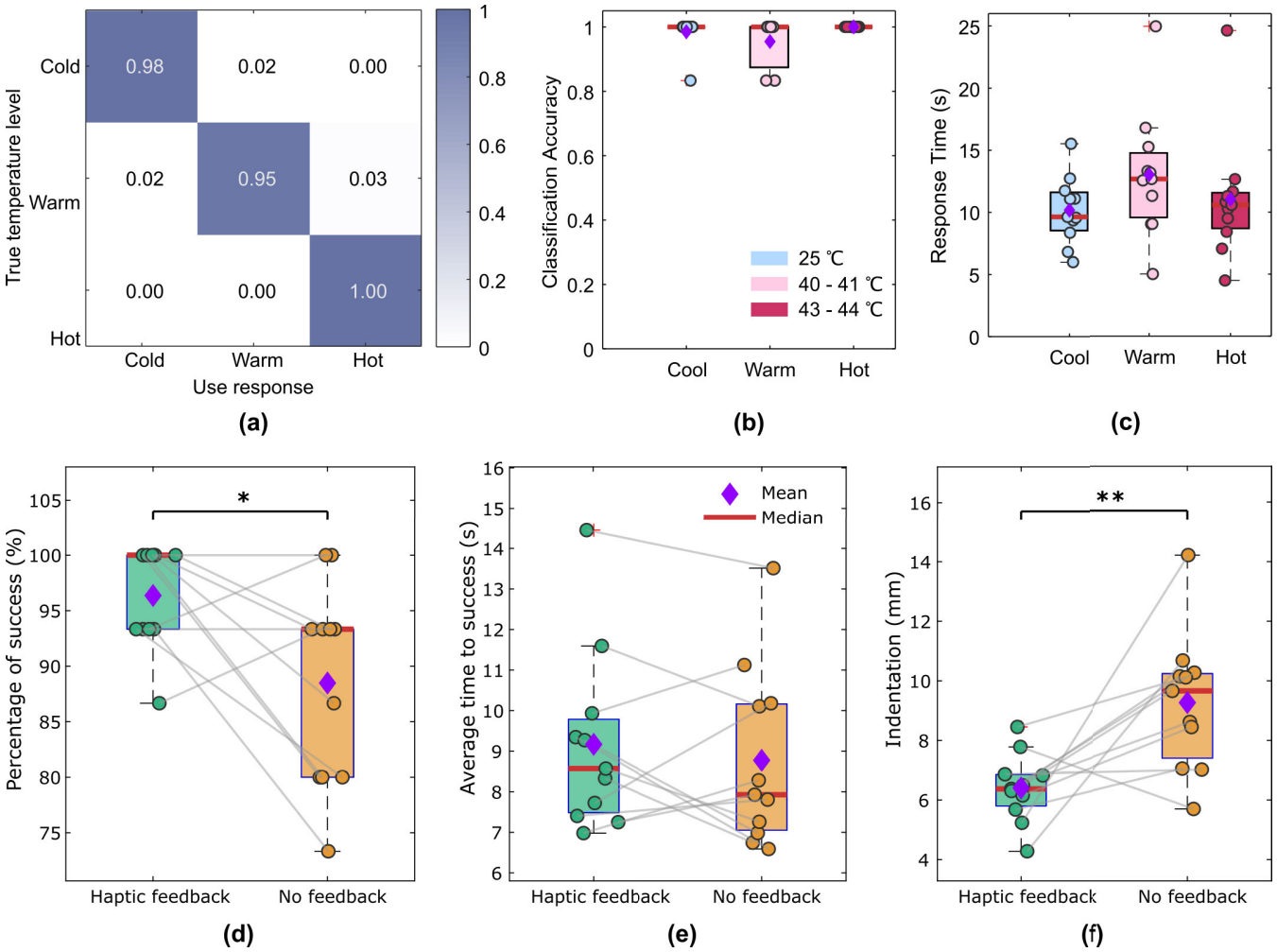

FIGURE 6. User study results: (a) temperature identification confusion matrix, (b) temperature classification accuracy by category, (c) response time distribution for temperature levels, (d) task success rate comparison, (e) average completion time comparison, (f) finger indentation comparison between haptic conditions.

order was randomized to minimize learning effects (see supplementary video).

Data collection encompassed task completion time, per-trial duration, failed attempts, and finger indentations. Measured metrics included success rate (success trials divided by total trials), average time to success (total time divided by success trials), and average indentation (mean index and thumb indentation when fingers were colliding with the cube). Statistical analysis employed paired t-tests between conditions (normality of paired differences was confirmed using the Shapiro–Wilk test when $p > 0.05$).

IV. EXPERIMENTAL RESULTS

A. THERMAL FEEDBACK PERFORMANCE

Temperature identification achieved high overall accuracy of 0.98 across all conditions, as shown in Fig. 6(a) and (b). Individual temperature accuracies were 0.98 (cool), 0.95 (warm), and 1.0 (hot). Median accuracy reached 1.0 across all temperature levels despite occasional classification errors in cool and warm conditions.

Response times varied by temperature level: mean values were 10.2 s (cool), 13 s (warm), and 11 s (hot), with an overall mean of 11.41 s (Fig. 6(c)). Response times included heating duration, subject identification period, and response recording time. The slightly longer response time for warm temperatures may reflect the intermediate nature of this thermal stimulus, requiring more deliberative discrimination.

B. HAPTIC FEEDBACK PERFORMANCE

Virtual manipulation results (Fig. 6(d)-(f)) demonstrated significant benefits of haptic feedback on task performance. The averaged success rates increased from 88.5% (NF) to 96.4% (HF), with statistical significance ($p = 0.029$), indicating that haptic feedback substantially enhances task completion reliability.

Task completion times showed no significant difference between conditions: averaged times to success were 8.8 s (NF) versus 9.2 s (HF) ($p = 0.455$). This can be explained by the fact that while haptic feedback provides additional

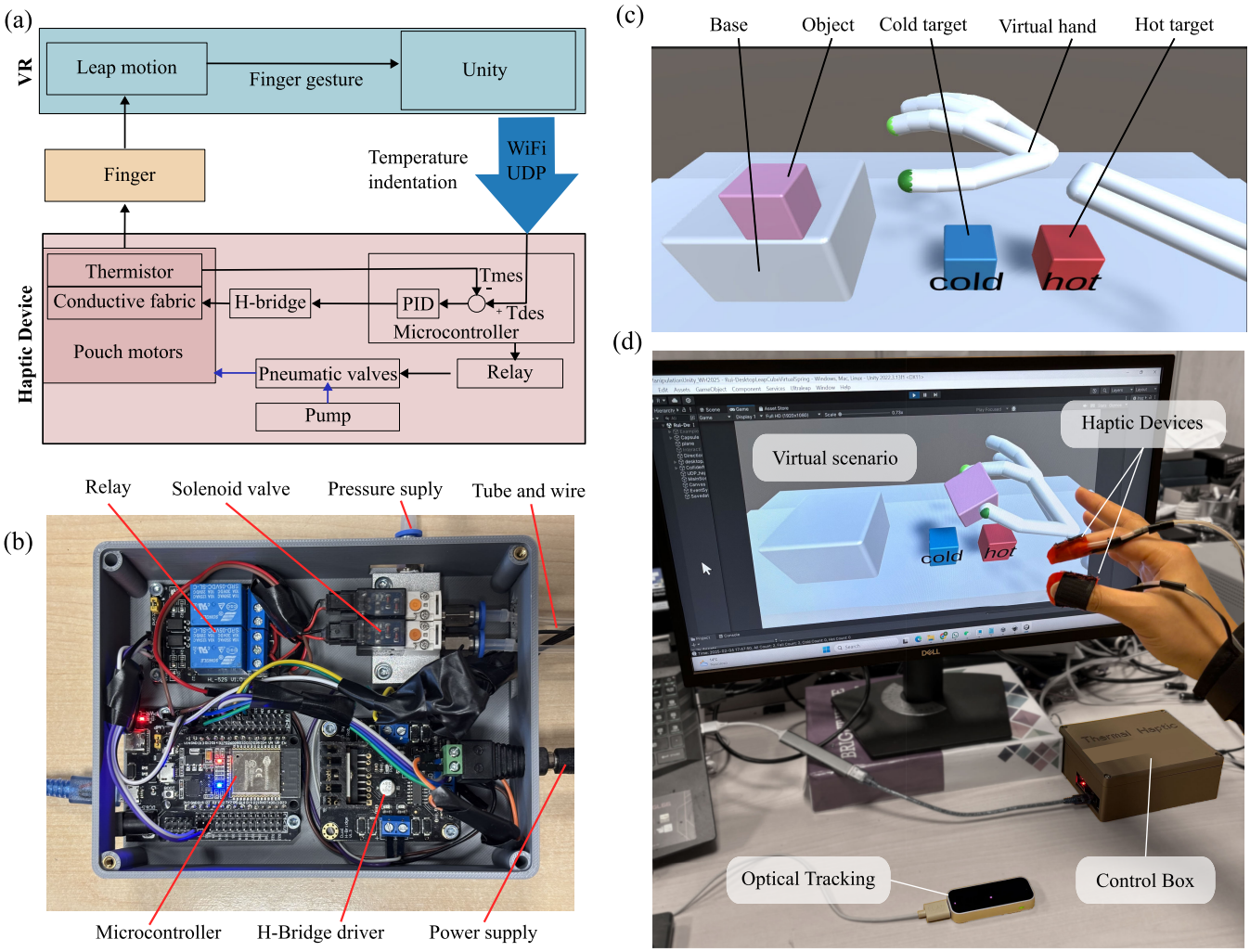

FIGURE 7. Experimental setup for combined thermal and haptic feedback. (a) Schematic diagram of the system. (b) Components in the control box. (c) Components in the VR environment. (d) Experimental setup for subjects.

informative sensory cues, hence improving grasping modulation and success rate, such information needs to be processed by the user, limiting or counterbalancing its impact on execution time.

Finger indentation analysis revealed significant behavioral differences ($p = 0.01$). The haptic feedback condition resulted in reduced average indentations of 6.4 mm compared to 9.3 mm without haptic feedback. This finding indicates that haptic feedback enables more controlled and gentle object manipulation, suggesting improved force modulation and spatial awareness during virtual object interaction.

V. DISCUSSION

In this work, we presented a fully fabric-based approach to designing a wearable fingertip haptic device. By integrating thermal features directly within the pneumatic structure, our approach differs from other pneumatic wearable devices by enabling congruent multimodal feedback with reduced complexity and faster response compared to other pneumatic or fluid-based systems [26], [27]. The fully fabric construction achieves ultra-lightweight actuation at only 2 g per module, substantially lighter than haptic devices using conventional electromagnetic motors [30], [32], while providing enhanced wearability and mobility compared to desktop thermal interfaces [34]. The soft fabric heaters overcome the inherent rigidity limitations of conventional Peltier-based thermal systems [33], [35] and demonstrate superior flexibility (please see supplementary video) compared to flexible thermoelectric devices [37], [38], [39], [40].

The characterization studies reveal a critical trade-off between thermal and force performance in finger-actuator clearance design. Enhanced cooling rates observed when the finger is not in contact with the actuator suggest that increased fingerpad-actuator clearance could accelerate cooling during deflated states. However, increased clearance correspondingly reduces force output capabilities. Despite the challenge of precise clearance adjustment, our analysis indicates that a 2 mm clearance represents an optimal compromise, maintaining 86% of maximum force output while significantly improving thermal responsiveness.

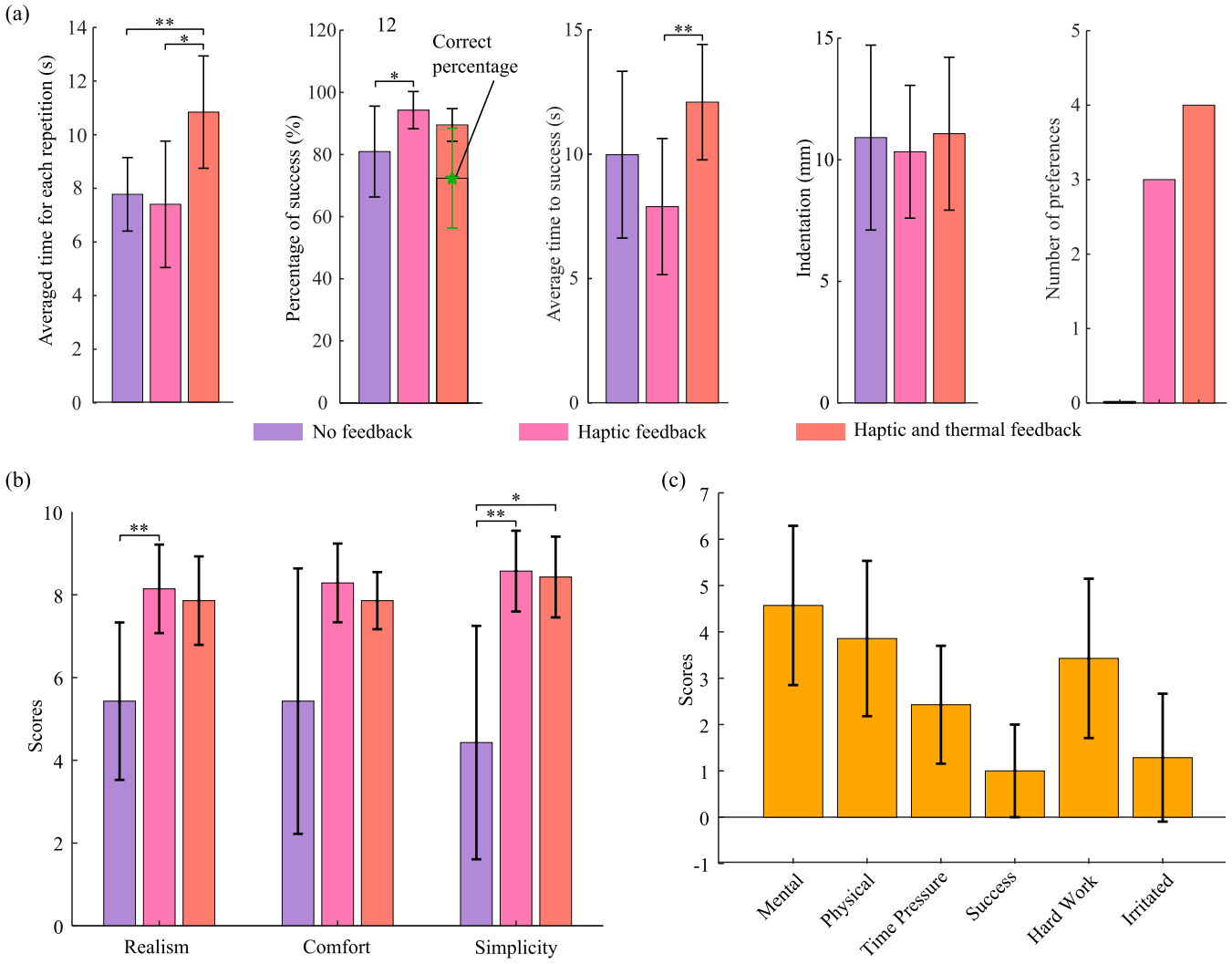

FIGURE 8. Results of combined thermal and haptic feedback testing. (a) Performance metrics comparison across three conditions. (b) Subjective evaluation scores for each condition. (c) NASA-TLX workload assessment.

Two user studies validated the device's functionality through complementary approaches. A user study integrated thermal and haptic feedback within a VR manipulation task (detailed in Appendix A), while separate studies evaluated temperature identification and virtual manipulation to validate individual modality performance. These studies demonstrate the device's effectiveness across different interaction paradigms. It should be noted that in the experimental comparison, the No Haptic condition was performed with bare hands, differing from the conventional procedure of just disabling the haptic device. Hence, the improved performance in the Haptic condition already includes any possible effect on dexterity that wearing the haptic interface may involve.

Subtle differences between study protocols yield insights into system optimization. The virtual manipulation protocol comparison reveals that proportional pressure control (matching indentation to pressure) achieves superior force regulation compared to binary on-off control. This is evidenced by greater and more significant indentation reduction with haptic feedback under proportional control (Fig. 6(f)) versus on-off control (Fig. 8(a), Appendix A), indicating more precise force modulation capabilities.

Temperature feedback evaluation demonstrates context-dependent performance characteristics. In isolated temperature identification tasks, subjects exhibited deliberative behavior with extended response times (11.41 s overall) but achieved high accuracy (0.98 overall). Conversely, the preliminary experiment (included in Appendix A) with integrated thermal-haptic VR manipulation showed that thermal discrimination, conducted alongside the pick-and-place task, carried minimal temporal overhead (3.06 s increase compared to haptic-only conditions), suggesting effective multimodal integration.

Several limitations warrant future investigation. First, while the pneumatic actuators and thermal sensors operated reliably throughout our user studies (over 700 inflation and 300 thermal cycles, respectively, without failures), comprehensive fatigue testing under extended operational conditions remains to be conducted. Second, the pilot user

studies (n=11, 7 male/4 female) provide initial device validation but have limited statistical power for broader generalization; larger-scale studies are needed to establish population-level findings and investigate potential demographic factors such as gender effects on haptic perception and device performance. Third, the passive cooling time represents a significant constraint for VR applications requiring rapid thermal transitions. In our user studies, participants were required to wait approximately 20 seconds between trials to ensure clear perception of subsequent thermal changes, which would pose substantial challenges for real-time VR applications. Active cooling mechanisms (e.g., miniature Peltier modules, forced air cooling, or phase-change materials) will be necessary in future iterations to cope with more demanding application requirements. Fourth, observed latency between VR interaction and pneumatic actuation (visible in supplementary video) requires systematic characterization and optimization. The total system latency is estimated in approximately 0.33 s, comprising hand tracking frame rate (∼8 ms from manufacturer data), virtual physical simulation rate (∼17 ms), WiFi UDP communication to the device (∼5 ms from roundtrip test), and pneumatic response (∼300 ms). Fifth, while conductive fabric offers flexibility and lightweight advantages, alternative materials, including copper foil, liquid metal circuits, or conductive yarns, merit investigation for enhanced thermal performance. Finally, additional rendering techniques (i.e., vibration modulation) can provide additional tactile dimensions or alternative force rendering approaches, necessitating comparative evaluation in similar fine manipulation scenarios.

VI. CONCLUSION

This study presents a novel lightweight fabric-based thermal haptic device for human-machine interaction, envisaging applications in virtual reality interactions. The device integrates fabric-based electric heating and pneumatic actuation to deliver congruent thermal and haptic feedback to fingertips. Weighing only 2 g per thimble, the system achieves force output up to 8.93 N at 50 kPa with rapid thermal response (3°C/s peak heating rate).

Characterization studies establish optimal design parameters, identifying 2 mm clearance as the ideal compromise, maintaining 86% of maximum force while enhancing thermal responsiveness. User studies validate device effectiveness: temperature identification achieved 98% accuracy, while virtual manipulation showed significant improvements in task success rates (88.5% to 96.4%, $p = 0.029$) and force control precision ($p = 0.01$). Another pilot user study showed similar benefits with combined thermal-haptic feedback delivered in a similar manipulation task. Noticeably, improved performance was achieved versus a bare-hands No Feedback condition, highlighting the wearability and preservation of the user's dexterity of the proposed approach.

APPENDIX A
USER STUDY: COMBINED THERMAL AND HAPTIC FEEDBACK

A. EXPERIMENTAL SETUP AND PROTOCOL

This user study was conducted to evaluate the integrated performance of thermal and haptic feedback within a unified VR manipulation task. The system architecture, shown in Fig. 7(a) and (b), follows the same basic configuration described in Section III of the main text. However, two key modifications were implemented to investigate different aspects of multimodal feedback integration.

First, the pneumatic actuation strategy differs from the main experiments: haptic feedback employs an **on-off** control scheme rather than proportional pressure modulation. Specifically, pneumatic valves deliver a constant 8 kPa pressure when finger indentation exceeds a predefined threshold and remain inactive otherwise. This binary control approach establishes a baseline for evaluating the advantages of proportional control implemented in the main study.

Second, the VR environment (Fig. 7(c) and (d)) incorporates two color-coded targets—a blue target representing cold objects and a red target for hot objects—instead of the single target used in the main experiments. This dual-target configuration enables investigation of temperature-based decision-making during object manipulation tasks. The purple cube object and virtual hand interaction mechanics (using proxy points, virtual springs, and collision spheres) remain consistent with the description in Section III-C.

Seven healthy subjects (5 male, 2 female; aged 22–33 years) participated in this study following informed consent procedures approved by the ethical board of the Scuola Superiore Sant'Anna (protocol 412023). Each subject completed 15 trials under three experimental conditions with distinct task requirements:

- **No Feedback (NF)**: Subjects manipulated the virtual object with visual feedback only, without any haptic or thermal cues. To standardize movement distance across trials, subjects alternated placement between the blue and red targets.
- **Haptic Feedback (HF)**: Subjects received binary tactile feedback (8 kPa activation above indentation threshold) without temperature rendering. Similar to the NF condition, subjects alternated placement between the two targets to maintain consistent movement distance.
- **Haptic and Temperature Feedback (HTF)**: Subjects received both tactile and thermal feedback. Critically, the task requirements differed from the previous two conditions: the virtual object's temperature was randomly assigned to either 20°C (cold) or 40°C (hot) for each trial with equal probability. Subjects were required to identify the object's temperature through tactile thermal sensing and place it on the corresponding color-coded target (blue for cold, red for hot). Incorrect target placement was counted as a failed trial, regardless of object stability.

Subjects were instructed to grasp the object and place it on one of the two targets for 15 trials in each condition. Successful placement required keeping the object stationary on the target for 1.5 seconds (Fig. 5(d)). If the object fell to the ground, it was counted as a failed attempt. In the first two conditions, subjects alternated between the two targets to standardize the movement distance. In the third condition, the object's temperature was randomly assigned as either 20°C (cold) or 40°C (hot) in each attempt, corresponding to the blue or red targets, respectively. Theoretically, the probability of being assigned to both temperatures is 50%. Subjects had to identify the object's temperature and place it on the correct target (blue for cold, red for hot).

B. DATA COLLECTION AND STATISTICAL ANALYSIS

Data collection followed the same framework as the main study, including total task completion time, per-trial duration, number of failed attempts, and finger indentations. For the HTF condition, temperature identification accuracy was additionally recorded based on correct target selection. Performance metrics were calculated identically: averaged time per trial (total time / 15), success rate ((15 - failed attempts) / 15), averaged time to success (total time / number of successful trials), and average indentation (mean index and thumb indentation during object contact).

This study incorporated two post-experiment questionnaires to assess subjective experience, which were not administered in the main experiments:

Subjective Experience Questionnaire: Participants rated their experience across the three conditions using 10-point Likert scales (0 = very difficult/uncomfortable/unrealistic; 10 = very easy/comfortable/realistic). The questionnaire evaluated:

- Q1–Q3: Task ease, overall comfort, and perceived realism without haptic feedback
- Q4–Q6: Task ease, overall comfort, and perceived realism with haptic feedback
- Q7–Q9: Task ease, overall comfort, and perceived realism with combined haptic and temperature feedback
- Q10: Overall preference among the three conditions

Responses to Q1–Q9 were aggregated into three evaluation dimensions: realism, comfort, and simplicity. Mean scores and standard deviations were computed across all seven subjects for each dimension.

NASA Task Load Index (NASA-TLX): Participants assessed perceived workload across six standard dimensions (mental demand, physical demand, temporal demand, performance, effort, and frustration) using 0–10 scales, where lower scores indicate reduced task difficulty and workload.

C. EXPERIMENTAL RESULTS

Performance results, presented in Fig. 8(a), reveal distinct patterns across experimental conditions. Average time per trial was 7.74 s (NF), 7.37 s (HF), and 10.8 s (HTF). The HTF condition exhibited significantly longer completion times compared to both NF ($p = 0.007$) and HF ($p = 0.013$). This 3.43 s increase from HF to HTF primarily reflects the additional cognitive and temporal demands of temperature discrimination, combined with the physical heating time required to reach 40°C and subsequent passive cooling between trials with different temperature assignments.

Task success rates demonstrated substantial benefits from haptic feedback: 81% (NF) increased significantly to 94% (HF, $p = 0.045$), with an average of only one failure across 15 trials. The HTF condition achieved an 89.5% success rate while maintaining 80.9% temperature recognition accuracy, validating the effectiveness of thermal feedback integration despite the dynamic nature of the discrimination task conducted during object manipulation. Averaged time to complete successful trials was 10 s (NF), 7.9 s (HF), and 12 s (HTF), reflecting both improved efficiency with haptic feedback and added complexity with thermal discrimination requirements.

Average finger indentation exhibited minimal variation across conditions: 10.9 mm (NF), 10.3 mm (HF), and 11.1 mm (HTF), with no statistically significant differences. This finding contrasts markedly with results from the main study (Section IV-B), where proportional pressure control produced more pronounced indentation differences between conditions (9.3 mm without feedback vs. 6.4 mm with haptic feedback). The absence of significant indentation modulation under binary on-off control suggests that proportional pressure regulation enables substantially more refined force control and tactile awareness compared to simple threshold-based actuation.

Subject preference results provided clear evidence that feedback modalities enhance user experience: 4 participants selected HTF as their preferred condition, 3 chose HF, while no participants preferred NF.

D. SUBJECTIVE EVALUATION

Subjective evaluation results (Fig. 8(b)) strongly support the effectiveness of multimodal feedback. Both HF and HTF conditions received consistently high ratings across all evaluation dimensions, averaging approximately 8/10 for realism, comfort, and ease of use. In contrast, the NF condition yielded substantially lower scores (approximately 5/10), indicating diminished perceived realism, reduced comfort, and increased task difficulty.

Statistical analysis confirmed these observations with significant differences in multiple dimensions. Realism scores differed significantly between NF and HF ($p = 0.002$). The simplicity dimension showed significant differences for both NF versus HF ($p = 0.004$) and NF versus HTF ($p = 0.0134$), demonstrating that both haptic and thermal feedback contribute meaningfully to enhancing user perceptual experience and interaction quality.

NASA-TLX results (Fig. 8(c)) indicated consistently low perceived workload across all experimental conditions, with participants reporting average scores of approximately 2.5/10 for both mental and physical demands. These low

workload ratings confirm that the observed performance differences reflect genuine effects of feedback modality rather than confounding factors such as excessive cognitive load, physical fatigue, or time pressure. The uniformly low workload scores across conditions validate that the experimental tasks were appropriately calibrated to isolate feedback effects while maintaining ecological validity.

ACKNOWLEDGMENT

The authors would like to thank the participants in their user study for their time and dedication. They also acknowledge valuable discussions with colleagues in the field of haptic interfaces and soft robotics that helped shape this research.

REFERENCES

[1] A. Frisoli and D. Leonardis, "Wearable haptics for virtual reality and beyond," *Nature Rev. Electr. Eng.*, vol. 1, no. 10, pp. 666–679, Sep. 2024.

[2] N. T. Tanacar, M. H. Mughrabi, A. U. Batmaz, D. Leonardis, and M. Sarac, "The impact of haptic feedback during sudden, rapid virtual interactions," in *Proc. IEEE World Haptics Conf. (WHC)*, Jul. 2023, pp. 64–70.

[3] H. Bai, S. Li, and R. F. Shepherd, "Elastomeric haptic devices for virtual and augmented reality," *Adv. Funct. Mater.*, vol. 31, no. 39, Sep. 2021, Art. no. 2009364.

[4] C. Pacchierotti and D. Prattichizzo, "Cutaneous/tactile haptic feedback in robotic teleoperation: Motivation, survey, and perspectives," *IEEE Trans. Robot.*, vol. 40, pp. 978–998, 2024.

[5] H. A. Sonar, J.-L. Huang, and J. Paik, "Soft touch using soft pneumatic actuator–skin as a wearable haptic feedback device," *Adv. Intell. Syst.*, vol. 3, no. 3, Mar. 2021, Art. no. 2000168.

[6] A. Adilkhanov, M. Rubagotti, and Z. Kappassov, "Haptic devices: Wearability-based taxonomy and literature review," *IEEE Access*, vol. 10, pp. 91923–91947, 2022.

[7] R. Chen, D. Leonardis, A. Frisoli, and D. Chiaradia, "A powerful customized fabric-based soft robotic glove for assistance and rehabilitation," in *Proc. Int. Conf. Rehabil. Robot. (ICORR)*, May 2025, pp. 669–674.

[8] R. Chen, A. Frisoli, and D. Chiaradia, "Lateral pleated pneumatic artificial muscles: High-contraction and extended high-force range actuators for soft robotics," *IEEE/ASME Trans. Mechatronics*, vol. 31, no. 1, pp. 523–533, Feb. 2026.

[9] H. Choi, M. R. Cutkosky, and A. A. Stanley, "Integrated pneumatic sensing and actuation for soft haptic devices," *IEEE Robot. Autom. Lett.*, vol. 8, no. 11, pp. 7591–7598, Nov. 2023.

[10] S. Cai, Z. Chen, H. Gao, Y. Huang, Q. Zhang, X. Yu, and K. Zhu, "ViboPneumo: A vibratory-pneumatic finger-worn haptic device for altering perceived texture roughness in mixed reality," *IEEE Trans. Vis. Comput. Graph.*, vol. 31, no. 7, pp. 3957–3972, Jul. 2025.

[11] J. Qi, F. Gao, G. Sun, J. C. Yeo, and C. T. Lim, "HaptGlove—Untethered pneumatic glove for multimode haptic feedback in reality–virtuality continuum," *Adv. Sci.*, vol. 10, no. 25, Sep. 2023, Art. no. 2301044.

[12] F. E. V. Beek, Q. P. I. Bisschop, and I. A. Kuling, "Validation of a soft pneumatic unit cell (PUC) in a VR experience: A comparison between vibrotactile and soft pneumatic haptic feedback," *IEEE Trans. Haptics*, vol. 17, no. 2, pp. 191–201, Apr. 2024.

[13] A. Talhan, Y. Yoo, and J. R. Cooperstock, "Soft pneumatic haptic wearable to create the illusion of human touch," *IEEE Trans. Haptics*, vol. 17, no. 2, pp. 177–190, Apr. 2024.

[14] R. Niiyama, D. Rus, and S. Kim, "Pouch motors: Printable/inflatable soft actuators for robotics," in *Proc. IEEE Int. Conf. Robot. Autom. (ICRA)*, May 2014, pp. 6332–6337.

[15] R. Niiyama, X. Sun, C. Sung, B. An, D. Rus, and S. Kim, "Pouch motors: Printable soft actuators integrated with computational design," *Soft Robot.*, vol. 2, no. 2, pp. 59–70, Jun. 2015.

[16] M. Raitor, J. M. Walker, A. M. Okamura, and H. Culbertson, "WRAP: Wearable, restricted-aperture pneumatics for haptic guidance," in *Proc. IEEE Int. Conf. Robot. Autom. (ICRA)*, May 2017, pp. 427–432.

[17] W. Wu and H. Culbertson, "Wearable haptic pneumatic device for creating the illusion of lateral motion on the arm," in *Proc. IEEE World Haptics Conf. (WHC)*, Jul. 2019, pp. 193–198.

[18] S. Yamaguchi, T. Hiraki, H. Ishizuka, and N. Miki, "Handshake feedback in a haptic glove using pouch actuators," *Actuators*, vol. 12, no. 2, p. 51, Jan. 2023.

[19] J. Lee, D. Kim, H. Sul, and S. H. Ko, "Thermo-haptic materials and devices for wearable virtual and augmented reality," *Adv. Funct. Mater.*, vol. 31, no. 39, Sep. 2021, Art. no. 2007376.

[20] A. Raza, W. Hassan, and S. Jeon, "Pneumatically controlled wearable tactile actuator for multi-modal haptic feedback," *IEEE Access*, vol. 12, pp. 59485–59499, 2024.

[21] Q. Yan and M. G. Kanatzidis, "High-performance thermoelectrics and challenges for practical devices," *Nature Mater.*, vol. 21, no. 5, pp. 503–513, May 2022.

[22] S. H. Ko and J. Rogers, "Functional materials and devices for Xr (Vr/Ar/Mr) applications," 2021, Art. no. 2106546. [Online]. Available: https://advanced.onlinelibrary.wiley.com/doi/abs/10.1002/adfm.202106546

[23] J. Oh, S. Kim, S. Lee, S. Jeong, S. H. Ko, and J. Bae, "A liquid metal based multimodal sensor and haptic feedback device for thermal and tactile sensation generation in virtual reality," *Adv. Funct. Mater.*, vol. 31, no. 39, Sep. 2021, Art. no. 2007772.

[24] Y. Visell, "Tactile sensory substitution: Models for enaction in HCI," *Interacting Comput.*, vol. 21, nos. 1–2, pp. 38–53, Jan. 2009.

[25] D. M. Eagleman and M. V. Perrotta, "The future of sensory substitution, addition, and expansion via haptic devices," *Frontiers Human Neurosci.*, vol. 16, Jan. 2023, Art. no. 1055546.

[26] D. T. Goetz, D. K. Owusu-Antwi, and H. Culbertson, "PATCH: Pump-actuated thermal compression haptics," in *Proc. IEEE Haptics Symp. (HAPTICS)*, Mar. 2020, pp. 643–649.

[27] S. Cai, P. Ke, T. Narumi, and K. Zhu, "ThermAirGlove: A pneumatic glove for thermal perception and material identification in virtual reality," in *Proc. IEEE Conf. Virtual Reality 3D User Interface (VR)*, Mar. 2020, pp. 248–257.

[28] Y. Liu, S. Nishikawa, Y. A. Seong, R. Niiyama, and Y. Kuniyoshi, "ThermoCaress: A wearable haptic device with illusory moving thermal stimulation," in *Proc. CHI Conf. Human Factors Comput. Syst.*, May 2021, pp. 1–12, doi: 10.1145/3411764.3445777.

[29] M. K. Shilpa, M. Abdul Raheman, A. Aabid, M. Baig, R. K. Veeresha, and N. Kudva, "A systematic review of thermoelectric Peltier devices: Applications and limitations," *Fluid Dyn. Mater. Process.*, vol. 19, no. 1, pp. 187–206, 2023.

[30] M. Gabardi, D. Leonardis, M. Solazzi, and A. Frisoli, "Development of a miniaturized thermal module designed for integration in a wearable haptic device," in *Proc. IEEE Haptics Symp. (HAPTICS)*, Mar. 2018, pp. 100–105.

[31] J.-H. Kim et al., "A wirelessly programmable, skin-integrated thermo-haptic stimulator system for virtual reality," *Proc. Nat. Acad. Sci. USA*, vol. 121, no. 22, May 2024, Art. no. 2404007121.

[32] S. Kang, G. Kim, S. Hwang, J. Park, A. I. A. M. Elsharkawy, and S. Kim, "Flip-pelt: Motor-driven Peltier elements for rapid thermal stimulation and congruent pressure feedback in virtual reality," in *Proc. 37th Annu. ACM Symp. User Interface Softw. Technol.*, Oct. 2024, pp. 1–15, doi: 10.1145/3654777.3676363.

[33] B. Zhang and M. Sra, "PneuMod: A modular haptic device with localized pressure and thermal feedback," in *Proc. 27th ACM Symp. Virtual Reality Softw. Technol.*, Dec. 2021, pp. 1–7, doi: 10.1145/3489849.3489857.

[34] E.-H. Lee, S.-H. Kim, and K.-S. Yun, "Three-axis pneumatic haptic display for the mechanical and thermal stimulation of a human finger pad," *Actuators*, vol. 10, no. 3, p. 60, Mar. 2021.

[35] S. Lee, S. Jang, and Y. Cha, "Soft wearable thermo+touch haptic interface for virtual reality," *iScience*, vol. 27, no. 12, Dec. 2024, Art. no. 111303.

[36] L. A. Nimmagadda, R. Mahmud, and S. Sinha, "Materials and devices for on-chip and off-chip Peltier cooling: A review," *IEEE Trans. Compon., Packag., Manuf. Technol.*, vol. 11, no. 8, pp. 1267–1281, Aug. 2021.

[37] S.-W. Kim, S. H. Kim, C. S. Kim, K. Yi, J.-S. Kim, B. J. Cho, and Y. Cha, "Thermal display glove for interacting with virtual reality," *Sci. Rep.*, vol. 10, no. 1, p. 11403, Jul. 2020.

[38] S. Hong, Y. Gu, J. K. Seo, J. Wang, P. Liu, Y. S. Meng, S. Xu, and R. Chen, "Wearable thermoelectrics for personalized thermoregulation," *Sci. Adv.*, vol. 5, no. 5, p. 0536, May 2019.

[39] S. Kim, T. Kim, C. S. Kim, H. Choi, Y. J. Kim, G. S. Lee, O. Oh, and B. J. Cho, "Two-dimensional thermal haptic module based on a flexible thermoelectric device," *Soft Robot.*, vol. 7, no. 6, pp. 736–742, Dec. 2020, doi: 10.1089/soro.2019.0158.

[40] A. Nasser, K.-N. Keng, and K. Zhu, "ThermalCane: Exploring thermotactile directional cues on cane-grip for non-visual navigation," in *Proc. 22nd Int. ACM SIGACCESS Conf. Comput. Accessibility*, Oct. 2020, pp. 1–12.
[41] C. Pacchierotti, S. Sinclair, M. Solazzi, A. Frisoli, V. Hayward, and D. Prattichizzo, "Wearable haptic systems for the fingertip and the hand: Taxonomy, review, and perspectives," *IEEE Trans. Haptics*, vol. 10, no. 4, pp. 580–600, Oct. 2017.
[42] H. Hsiao, J. Whitestone, T.-Y. Kau, and B. Hildreth, "Firefighter hand anthropometry and structural glove sizing: A new perspective," *Human Factors*, vol. 57, no. 8, pp. 1359–1377, Dec. 2015.
[43] B. G. Green, "Temperature perception and nociception," *J. Neurobiol.*, vol. 61, no. 1, pp. 13–29, Oct. 2004.
[44] D. Leonardis, M. Solazzi, I. Bortone, and A. Frisoli, "A 3-RSR haptic wearable device for rendering fingertip contact forces," *IEEE Trans. Haptics*, vol. 10, no. 3, pp. 305–316, Jul. 2017.

RUI CHEN (Student Member, IEEE) received the B.S. degree in mechanical engineering from Southwest Jiaotong University, the M.S. degree in product system engineering from RWTH Aachen University, and the M.S. degree in mechanical engineering from Tsinghua University. He is currently pursuing the Ph.D. degree in emerging digital technology with the Institute of Intelligent Mechanics, Sant'Anna School of Advanced Studies (SSSA). His research interests include inflatable actuators and soft wearable robots.

XIANLONG MAI received the B.Sc. degree in theoretical and applied mechanics from the University of Science and Technology of China, in 2021. He is currently pursuing the Ph.D. degree in instrument science and technology with the University of Science and Technology of China. His research interests include wearable exoskeletons, human–robot interaction, and teleoperation.

DOMENICO CHIARADIA received the M.S. degree (Hons.) in control theory and automation engineering from the Polytechnic University of Bari, Italy, in 2014, and the Ph.D. degree in perceptual robotics from the Sant'Anna School of Advanced Studies (SSSA), Pisa, Italy, in 2018. He is currently an Assistant Professor in mechanical engineering focusing on robotics with SSSA. He leads the group developing flexible and portable exoskeletons and soft exosuits in the human–robot interaction (HRI) research area. His current research interests include physical human–robot interaction, rigid and flexible exoskeletons and soft exosuits for assistance and rehabilitation, mechanical design and control of flexible joints, and haptic interfaces.

ANTONIO FRISOLI (Senior Member, IEEE) is currently a Full Professor of engineering mechanics and robotics with the Sant'Anna School of Advanced Studies (SSSA), Italy, where he leads the Human–Robot Interaction, Intelligence Mechanical Institute. He is also responsible for the SSSA macro node of the Artes4.0 competence center on collaborative robotics. He is very active in technology transfer and open innovation. He has been the Co-Founder of two spin-offs, such as Wearable Robotics srl and Next Generation Robotics srl. His research interests include collaborative, rehabilitation, and wearable robotics, exoskeletons, multimodal interaction and haptics, wearable devices, and virtual reality. He is an Associate Editor of *IEEE Robotics Automation Magazine* and covers several scientific and editorial roles in scientific societies, such as Eurohaptics and ICORR, international conferences, and international journals.

DANIELE LEONARDIS received the M.Sc. degree in automation engineering from the Polytechnic University of Bari, in 2009, and the Ph.D. degree in perceptual robotics from Sant'Anna School of Advanced Studies (SSSA), in 2015. He is currently an Assistant Professor in mechanical engineering at SSSA. He is a principal investigator of national and European research projects in the field of fine haptic feedback coupled to immersive virtual reality, experimented in rehabilitation, and teleoperation settings. His research interests include haptic feedback, telemanipulation, and wearable robotics applied to the clinical field.